Available online at www.sciencedirect.com
ScienceDirect
Trans. Nonferrous Met. Soc. China 20(2010) 82−89
Transactions of Nonferrous Metals Society of China
www.tnmsc.cn

Effect of grain size on corrosion behavior of electrodeposited bulk nanocrystalline Ni

QIN Li-yuan(秦丽元), LIAN Jian-she(连建设), JIANG Qing(蒋 青)

Key Laboratory of Automobile Materials of Ministry of Education, College of Materials Science and Engineering, Jilin University, Changchun 130025, China

Received 3 May 2009; accepted 5 September 2009

Abstract: Nanocrystalline (NC) and coarse-grained Ni with different grain sizes (from 16 nm to 2 μm) were fabricated by direct current electrodeposition. Effect of grain size on the electrochemical corrosion behavior of these Ni deposits in different corrosion media was characterized by using potentiodynamic polarization test, electrochemical impedance spectroscopy (EIS), X-ray photoelectron spectroscopy (XPS) and immersion corrosion test. Results show that in the NaOH or NaCl solution, the NC Ni exhibits improved corrosion resistance with the decrease of grain size. But in H_2SO_4 solution, the higher grain boundary density accelerates corrosion due to no passive process and the corrosion resistance of NC Ni decreases with refining grain size. The distinct experimental results of NC Ni in corrosion behavior can be reasonably explained by the positive or negative effect of high-density grain boundaries in different corrosion media.

Key words: Ni; nanocrystalline; electrodeposition; corrosion behavior; grain size

1 Introduction

Nanocrystalline (NC) materials are of great importance in industrial applications due to their unique properties, especially mechanical and chemical properties[1]. NC materials with comprehensive combination of excellent mechanical properties, increased corrosion resistance properties and good adhesion ability with substrate are considerably needed for design or operation of devices, machine and structural systems. Since NC materials are characterized by their high volume fraction of grain boundary which may comprise as much as 10%−30% of the total crystal volume[2], their corrosion behavior may be quite different from those of their coarse-grained (CG) counterparts. However, the corrosion behavior of NC metal has received only limited attention. A good understanding of the relation between the corrosion property of the NC materials and their microstructure is important for both prospective engineering applications and knowing of fundamental physicochemical properties[3].

Though recent developments in the synthesis method of NC materials have stimulated interest in understanding the corrosion resistance of NC materials, it is difficult to summarize and predict their corrosion properties. Actually, different synthesis methods give rise to difference in microstructure and properties of NC materials[4]. Previous reports[5−10] demonstrated that the corrosion behavior of NC metals varies in different metal systems and corrosion environments, which may depend on their nanostructure parameters, e.g., grain size. On the other hand, electrodeposited Ni has been widely used in many fields to improve surface finishing, corrosion resistance and wear properties[11−13]. But there have been few reports on the detailed corrosion behavior of electrodeposited NC Ni fabricated from a Watts bath. Therefore, in the present work, the corrosion behaviors of electrodeposited Ni with different grain sizes in three different corrosion media (NaOH, NaCl and H_2SO_4) were investigated using potentiodynamic polarization, impedance measurement techniques, X-ray photoelectron spectroscopy (XPS) and immersion corrosion test. The effects of grain size on the corrosion behavior of NC Ni were emphasized in comparison with

Foundation item: Project(2004CB619301) supported by the National Basic Research Program of China; Project(50871046) supported by the National Natural Science Foundation of China; Project supported by 985-Automotive Engineering of Jilin University, China
Corresponding author: LIAN Jian-she; Fax: +86-431-85095876; E-mail: lianjs@jlu.edu.cn
DOI: 10.1016/S1003-6326(09)60101-1

the corrosion behavior of conventional CG Ni.

2 Experimental

Bulk and fully dense Ni with a thickness of about 350 μm was prepared by direct current electrodeposition from an electrolyte containing nickel sulfate (about 200 g/L), nickel chloride (about 30 g/L), boric acid (about 30 g/L) and saccharin at a temperature of 50 ℃, a current density of 2.5 A/dm^2 and pH 5.0. The anode was pure Ni plate and the cathode was a steel sheet (C1008, AISI). The saccharin was added as a grain-refining agent during the deposition. Four Ni samples with different grain sizes were fabricated under the same condition by not adding or adding different amounts of saccharin (0.55, 0.65, 1.00 g/L) into the electrolyte. Crystallographic structure of the Ni deposits was studied by X-ray diffractometer (XRD, D/max 2500PC) with a Cu K_α radiation. Microstructures and grain sizes were observed using a transmission electron microscope (TEM, H−800).

The electrochemical measurement was carried out in a three-electrode cell with a platinum plate (Pt) as counter electrode and a saturated calomel electrode (SCE) as reference electrode using an electrochemical analyzer (VersaSTAT 3, AMWTEK). The Ni samples were used as working electrode. Measurement was performed in 10% NaOH, 3% NaCl and 1% H_2SO_4 aqueous solutions at room temperature (RT), respectively. All electrochemical tests were repeated at least twice. The electrodes and the samples were cleaned before the electrochemical test and then the samples were masked with lacquer except 1 cm^2 area exposed to the electrolyte. Before all the measurements, the samples were immersed into electrolyte for 30 min to stabilize the open-circuit potential (OCP), φ_0. Sweeping rates were 10 mV/s for the all potentiodynamic sweep experiments. The values of the corrosion potential (φ_{corr}) and the corrosion current density (J_{corr}) were calculated from the intersection of the cathodic and anodic Tafel curves extrapolated from the anodic and cathodic polarization curves. Measurements of electrochemical impedance spectra (EIS) were conducted at the OCP. The amplitude of applied potential was 10 mV and the frequency ranged from 0.01 Hz to 100 kHz. The measured frequency responses were interpreted using a non-linear least square fitting procedure with the help of commercial software ZSimpWin. The passive film formed on the NC Ni surface was investigated by X-ray photoelectron spectroscopy (XPS) on an ESCALAB MK II (VG) instrument. Al K_α (1486.6 eV) radiation was used as the excitation source.

To further confirm the corrosion resistance of the Ni samples with different grain sizes, immersion corrosion tests were conducted in the same solution as above electrochemical measurements at RT. The corrosion induced mass loss of the Ni samples at different time intervals was measured using a precision electronic balance (AE240 METTLER) with an accuracy of 0.01 mg. The mass loss of each sample was measured three times and the values were then averaged.

3 Results and discussion

3.1 Microstructure characteristics

The TEM images of the Ni deposits obtained from the baths with increasing saccharin concentration are shown in Fig.1. It can be seen that the grain size decreases with increasing the concentration of saccharin in the electrolyte[14]. The average grain sizes are about 2 μm, 258 nm, 93 nm and 16 nm for Ni deposits obtained from bath with saccharin concentration of 0, 0.55, 0.65 and 1.00 g/L, respectively. Those data were measured from a statistical analysis of the TEM images with about 300 grains of each sample. Because the grain size of Ni fabricated from the electrolyte without adding saccharin is in micrometer range, as shown in Fig.1(a), this kind of Ni is called CG Ni; and the others are called NC Ni.

The XRD patterns of the NC and CG Ni deposits are represented in Fig.2. All the specimens show single face-centered cubic (FCC) nickel phase and the growth orientation of the deposits gradually change from (200) plane to nearly random growth with decreasing grain size. The reason for the transition of the preferred orientation may result from the change of the surface energy of different growth planes induced by the addition of saccharin during electrodeposition[15]. In addition, the broadening of the diffraction peaks is observed, which can be attributed to the increase of crystalline imperfection like grain boundary and micro strain as grain size decreases[16].

3.2 Potentiodynamic polarization measurements and XPS analyses

Potentiodynamic polarization curves of the CG and NC Ni with different grain sizes in 10% NaOH, 3% NaCl and 1% H_2SO_4 aqueous solutions at RT are shown in Fig.3. All the Ni samples show an active-passive-transpassive behavior in the NaOH and NaCl solutions; however, they display only active behavior in H_2SO_4 solution. The detailed corrosion potentials and corrosion current densities of samples obtained from the electrochemical polarization curves are summarized in Table 1.

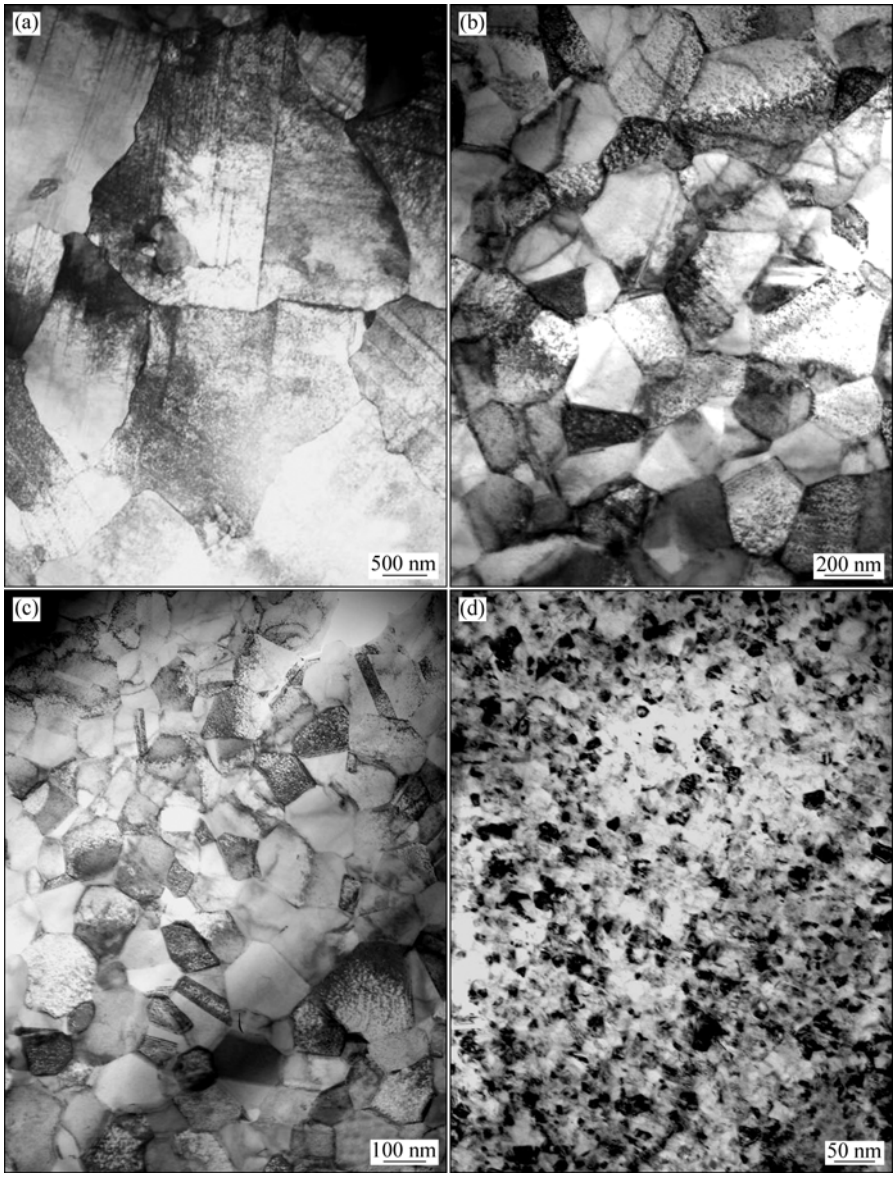

Fig.1 TEM images of Ni deposits obtained in electrolyte with different saccharin concentrations: (a) 0 g/L; (b) 0.55 g/L; (c) 0.65 g/L; (d) 1.00 g/L

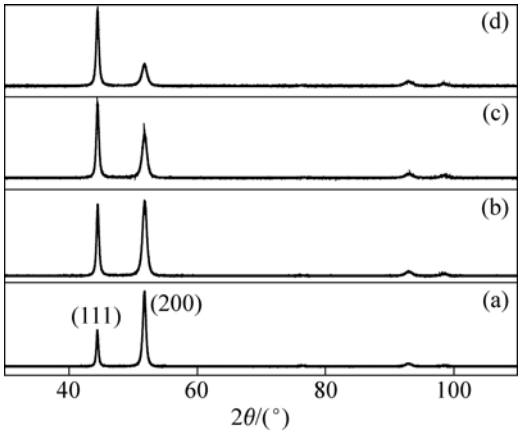

Fig.2 XRD patterns of Ni deposits with different grain sizes: (a) Coarse-grain, 2 μm; (b) Nanocrystalline, 258 nm; (c) Nanocrystalline, 93 nm; (d) Nanocrystalline, 16 nm

As seen from Fig.3(a) and Table 1, the corrosion potential shifts positively from −0.617 V to −0.429 V and the corrosion current density significantly decreases from 1.69 μA/cm^2 to 0.57 μA/cm^2 for the average grain size of the deposits decreases from 2 μm to 16 nm in NaOH solution. Moreover, 16 nm-Ni possesses the lowest passive current density (2.27 μA/cm^2) and the widest passive range (from −0.133 V to 0.198 V) among the Ni deposits. NaCl solution is a typical environment for the evaluating corrosion resistance of many materials. By utilizing the information in Fig.3(b) and Table 1, it can be observed that the corrosion potential of Ni deposits shifts negatively from −0.325 V to −0.494 V with decreasing grain size to 16 nm. But, the corrosion current density decreases evidently from 53.43 μA/cm^2 to 5.21 μA/cm^2 (10 times lower) as the average grain size

Table 1 Corrosion potential and corrosion current density of Ni deposits obtained from electrochemical polarization curves in 10% NaOH, 3% NaCl and 1% H_2SO_4 solutions

Solution	Sample	Corrosion potential (vs SCE)/V	Corrosion current density/(μA·cm^{-2})
1%NaOH	16 nm-Ni	−0.429	0.57
	93 nm-Ni	−0.470	0.79
	258 nm-Ni	−0.530	0.90
	2 μm-Ni	−0.617	1.69
3%NaCl	16 nm-Ni	−0.494	5.21
	93 nm-Ni	−0.462	7.55
	258 nm-Ni	−0.401	15.89
	2 μm-Ni	−0.325	53.43
1%H_2SO_4	16 nm-Ni	−0.084	45.19
	93 nm-Ni	−0.116	16.78
	258 nm-Ni	−0.184	7.73
	2 μm-Ni	−0.313	4.81

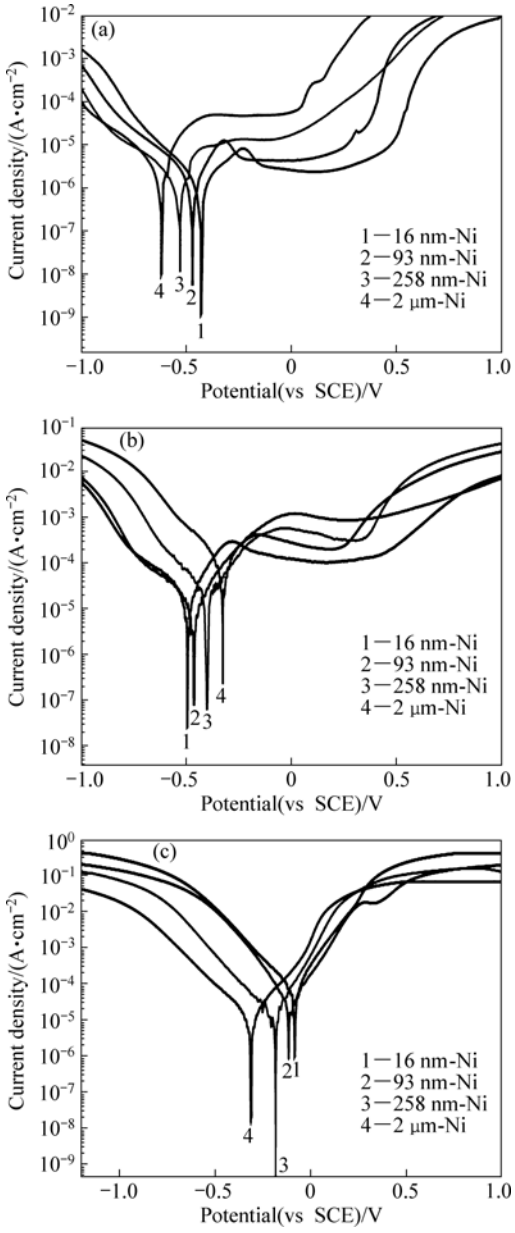

Fig.3 Potentiodynamic polarization curves of Ni deposits in 10% NaOH (a), 3% NaCl (b) and 1% H_2SO_4 solution (c)

decreases. Moreover, a lower passive current density and wider passive range are observed in 16 nm-Ni just as in NaOH solution. This indicates that NC Ni deposits with smaller grain size have higher density of nucleation sites for passive film, which leads to a higher fraction of passive layer, and thus a lower passive current density.

By considering all above features, it is concluded that the NC Ni with smaller grain size should exhibit better corrosion resistance in both 10% NaOH and 3% NaCl solutions. The enhanced corrosion resistance can be attributed to the formation of stable passive films on the surface of NC Ni samples. The passive films on 16 nm-Ni in NaOH and NaCl solutions were further confirmed by XPS surface analysis. Figs.4(a) and (b) show the high resolution XPS spectra of Ni $2p_{3/2}$ and O 1s, which were obtained from the 16 nm-Ni after being polarized at passive potential in the NaOH solution. The Ni $2p_{3/2}$ peaks decomposed into one main component located at a binding energy of (855.6±0.1) eV and its associated satellite of (861.4 ± 0.1) eV, which are attributed to $Ni(OH)_2$ on the surface[17−18]. Accordingly, the spectrum of O 1s is only one peak corresponding to the oxygen in $Ni(OH)_2$. Therefore, the XPS analysis indicates that the passive film formed on

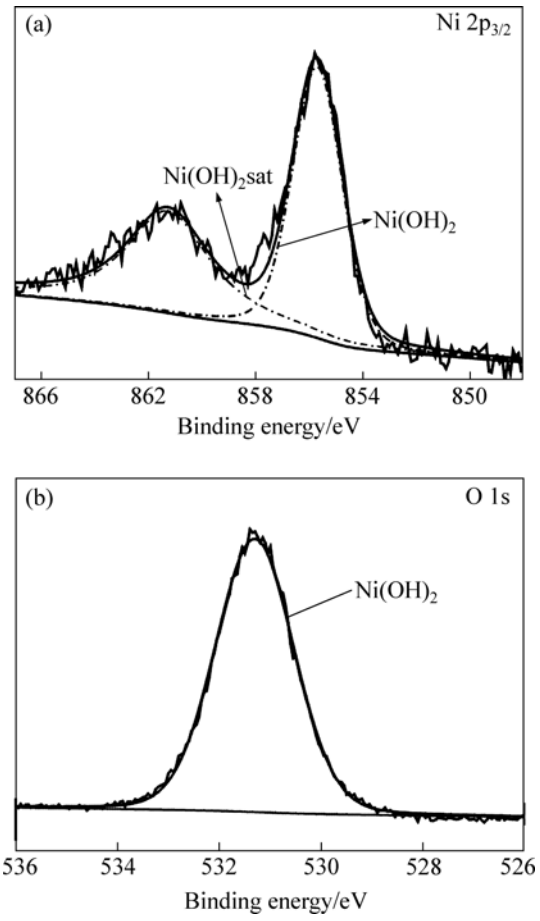

Fig.4 XPS spectra of Ni $2p_{3/2}$ (a) and O 1s (b) acquired from 16 nm-Ni after being polarized in 10% NaOH solution at 40 mV for 5 min

the NC Ni is composed of stable and continuous Ni hydroxide. The formation of $Ni(OH)_2$ passive film on the NC Ni surface in the anodic polarization stage may involve the following chemical and electrochemical steps[19]:

$$Ni+H_2O\rightarrow Ni(H_2O)(ads) \quad (1)$$

$$Ni(H_2O)(ads)\rightarrow Ni(OH)^+ + H^+ + 2e^- \quad (2)$$

$$Ni(OH)^+ + OH^- \rightarrow Ni(OH)_2 \quad (3)$$

Figs.5(a) and (b) show the Ni $2p_{3/2}$ and O 1s peaks respectively, which were obtained from the 16 nm-Ni after being polarized at passive potential in the NaCl solution. The Ni $2p_{3/2}$ peak consists of three main components, namely, metallic Ni, NiO and $Ni(OH)_2$[17, 20−22]. Similarly, the spectrum of O 1s in Fig.5(b) can be coherently fitted by two Gaussian components corresponding to the oxygen in $Ni(OH)_2$ and NiO. Hence, the passivation process of 16 nm-Ni in the NaCl solution involves the formation of both $Ni(OH)_2$ and NiO passive films. The former forms according to the above reactions (Eqs.(1)−(3)) and the latter involves another reaction[19]:

$$Ni(OH)_2\rightarrow NiO+H_2O \quad (4)$$

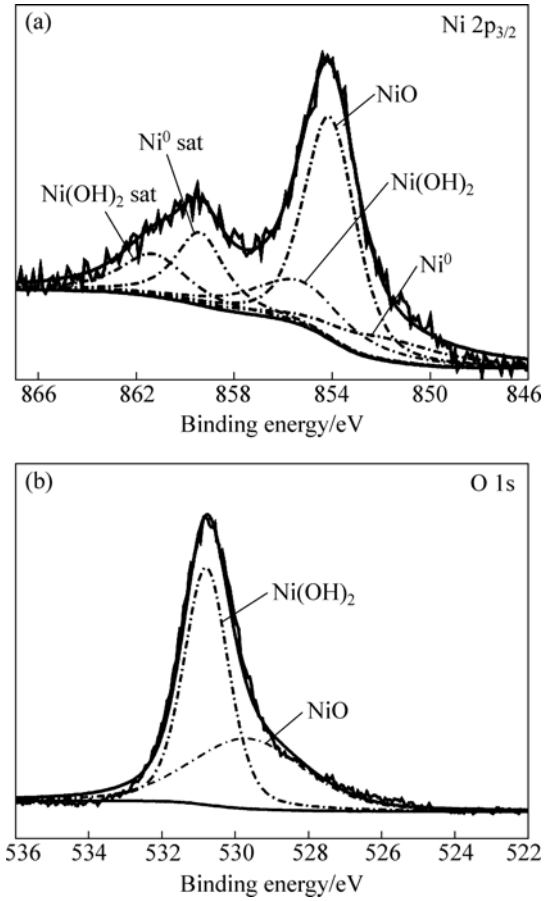

Fig.5 XPS spectra of Ni 2p3/2 (a) and O 1s (b) acquired from 16 nm-Ni after being polarized in 3% NaCl solution at 5 mV for 5 min

Fig.3(c) shows the polarization curves of the Ni samples in H_2SO_4 solution. The corrosion behavior is quite different from that in NaOH or NaCl solution as there is no obvious passivation phenomenon. The Ni sample with smaller grain size, e.g. 16 nm-Ni, exhibits more positive corrosion potential (−0.084 V). The positive shift of φ_{corr} noted in Fig.3(c) may be due to the catalysis of the hydrogen reduction process by the substantial quantity of crystalline defects (e.g., grain boundaries) on the surface. It is reported that reversible trapping of hydrogen at dislocations, grain boundaries and voids (pores) can change the kinetics of hydrogen evolution[9−10]. Therefore, the corrosion potential shifts positively with the decrease of grain size. However, all NC Ni samples exhibit higher corrosion current density than CG Ni, and the corrosion current density (45.19 $\mu A/cm^2$) of the 16 nm-Ni is 9 times higher than that (4.81 $\mu A/cm^2$) of the CG Ni sample. This can be understood as there is no passivation occurred in such strong corrosion media (1% H_2SO_4). In this case, plenty of grain boundaries in NC Ni surface provide more defect sites, which will increase the electro chemical reactivity and accelerate the corrosion of Ni[10].

3.3 EIS measurements

The Nyquist impedance plots, obtained for NC and CG Ni in 10% NaOH, 3% NaCl and 1% H_2SO_4 solutions at RT, are shown in Fig.6. The Nyquist plots of all the Ni deposits in NaOH solution (Fig.6(a)) exhibit a single semicircle at higher frequencies and the diameter of the semicircle increases evidently with decreasing grain size, indicating that the corrosion resistance of the Ni deposits increases with the decrease of grain size. In addition, a nearly ideal Warburg tail with an angle of 45° is obtained at lower frequencies, which corresponds to diffusion dominated process. Such a diffusion process indicates that the corrosion mechanism is controlled not only by the charge transfer but also by the diffusion process of some relative ions[17]. To account for the corrosion behavior of the Ni deposits in NaOH solution, an equivalent circuit model (inset of Fig.6(a)) has been proposed to simulate the metal/solution interface. Solution resistance, charge transfer resistance, Warburg impedance, and a constant phase element representing double-layer capacitance are used to fit the impedance data. The equivalent circuit model is based on the following equations:

$$Z(\omega)=R_s+Z_s/e(\omega) \quad (5)$$

$$Z_s/e(\omega)=\frac{1}{R_{ct}+Z(w)}+j\omega C \quad (6)$$

where ω, R_s, $Z_s/e(\omega)$, R_{ct}, C and $Z(w)$ are the angular frequency, solution resistance, impedance of solution/electrode interface, charge-transfer resistance, double-

layer capacitance and Warbrug diffusion impedance, respectively. In this model, $Z_s/e(\omega)$ represents the Faradic impedance as a result of the dissolution of Ni species in NaOH solution.

The formation of $Ni(OH)_2$ passive film confirmed by XPS analysis should provide the impedance at the electrolyte/passive film interface. Therefore, the above reactions can be modeled as a double-layer capacitor in parallel with R_{ct}. In addition, the corrosion rate is also affected by the inter-diffusion of Ni^{2+} and OH^-; and there should exist a Warburg diffusion element reasonably describing the diffusion effects of ions[23]. The calculated equivalent circuit parameters values are listed in Table 2. R_{ct} increases evidently with decreasing grain size, and R_{ct} of 16 nm-Ni is 3.4 times greater than that of the CG Ni. The decrease of CPE indicates the more smooth and protective nature of passive film formed on Ni deposits with decreasing grain size[5]. So, a better electrochemical corrosion resistance for NC Ni with smaller grain size is expected in NaOH solution.

Table 2 Equivalent circuit parameters determined by modeling impedance spectra of Ni deposits with different grain sizes in 10% NaOH, 3% NaCl and 1% H_2SO_4 solution

Solution	Sample	R_s/ ($\Omega\cdot cm^2$)	R_{ct}/ ($\Omega\cdot cm^2$)	Constant phase element/ ($\mu F\cdot cm^{-2}$)
10% NaOH	16 nm-Ni	2.32	5 130	39.41
	93 nm-Ni	2.46	3 840	45.38
	258 nm-Ni	2.04	2 238	48.75
	2 μm-Ni	2.82	1 497	50.09
3% NaCl	16 nm-Ni	13.95	6.441×10^5	6.13
	93 nm-Ni	12.93	2.854×10^5	4.85
	258 nm-Ni	12.63	1.905×10^5	4.27
	2 μm-Ni	11.67	9.421×10^4	6.17
1% H_2SO_4	16 nm-Ni	8.45	3 830	18.72
	93 nm-Ni	9.81	4 446	15.9
	258 nm-Ni	9.18	5 066	18.83
	2 μm-Ni	10.03	6 816	11.33

The measured impedance spectra for the Ni deposits in 3% NaCl and 1% H_2SO_4 solutions at RT are shown as the Nyquist impedance plots in Fig.6(b) and Fig.6(c), respectively. The Nyquist plots of all the Ni samples show only one capacitive loop in the entire frequency range. The unfinished semicircle arc is attributed to the charge transfer process in the electrode/electrolyte interface. Charge transfer resistance (R_{ct}) is the resistance offered by the metal atom to get ionized when in contact with the electrolyte. The larger the R_{ct} is, the higher the corrosion resistance of the sample is. In addition, constant phase element (CPE) is used as a substitute for double-layer capacitor to fit the impedance data of the interface between an electrode and the surrounding electrolyte. The simplified equivalent circuits shown in the insets of Figs.6(b) and (c) are used to model the electrode/electrolyte interface and the simulated results are listed in Table 2. As shown in Fig.6(b), the Nyquist plots of the Ni deposits in NaCl solution exhibit an increasing semicircle with decreasing grain size and the corresponding R_{ct} values also increase. R_{ct} value of 16 nm-Ni is 6.84 times larger than that of CG Ni. So, the

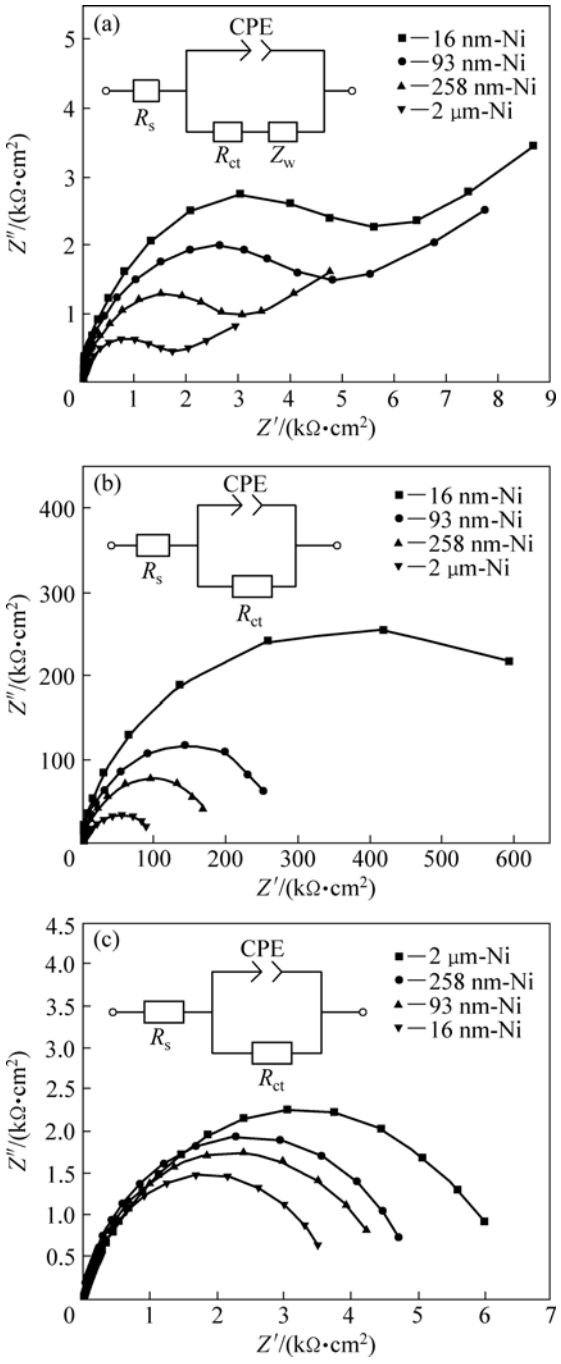

Fig.6 Nyquist impedance plots of Ni deposits in 10% NaOH (a), 3% NaCl (b) and 1% H_2SO_4 (c) solution after immersion for 30 min at their respective open circuit potentials(insets showing equivalent-circuit models for corrosion behavior of Ni deposits in above three kinds of corrosion media)

NC Ni with smaller grain size should exhibit better corrosion resistance in NaCl solution. However, the impedance plots of the Ni samples in 1% H_2SO_4 solution (Fig.6(c)) exhibit diminishing semicircle with decreasing grain size. R_{ct} value of 16 nm-Ni is the smallest among the Ni deposits, which implies the lowest corrosion resistance.

The above sequences of grain size influence on corrosion resistance are in agreement with those obtained from potentiodynamic polarization results. Passive film formation seems to be a dominant factor for the corrosion behavior of NC materials, which determines whether the higher grain boundary density and defect in NC materials provide positive or negative effects on the corrosion process. The improved corrosion resistance of NC Ni with smaller grain size in NaOH and NaCl solution can be explained as follows: Ni is a metal that can be passive easily, especially in alkaline solution. Since the passivation first starts on surface crystalline lattice defects and the smaller grain size NC Ni has higher density of grain boundaries and dislocations inside, the high fractions of grain boundaries will provide an increased number of active sites to quickly form a continuous and protective passive film[24]. The passive film increases the difficulty of Ni ions or electrons migrating toward the surface to participate electrochemical reaction. So, it is reasonable to conclude that the NC Ni with smaller grain size has a high fraction of passive layer and low corrosion rate due to a high density of nucleation sites for passive film. However, since there is obviously no passive process of the Ni samples in H_2SO_4 solution, the higher grain boundary density in NC Ni will accelerate corrosion by forming much more micro electrochemical cells between the huge amount of grain boundaries and the matrix, which increases the electrochemical reactivity during the corrosion process. As a result, the NC Ni with smaller grain size exhibits much higher corrosion rate and lower corrosion resistance in H_2SO_4 solution.

3.4 Immersion corrosion tests

For macroscopically and directly verifying the effect of grain size on corrosion resistance, the immersion corrosion tests were also conducted at RT. After immersing in 10% NaOH solution for 240 h, the mass loss of all samples is so slight that it can be almost ignored. All the samples maintain metallic luster and neither selective corrosion nor pitting corrosion could be observed on their surfaces. After being immersed in 3% NaCl and 1% H_2SO_4 solutions for 240 h, the mass losses of Ni deposits are shown in Fig.7(a) and Fig.7(b), respectively. The mass loss of CG Ni in 3% NaCl solution is 4.51 mg but that of 16 nm-Ni is only 0.31 mg, which indicates the better corrosion resistance of NC Ni in comparison with CG Ni deposits. However, in 1% H_2SO_4 solution, the NC Ni with smaller grain size dissolves more actively. The 16 nm-Ni shows the largest mass loss of 42.28 mg which is 5.3 times larger than that of the CG Ni sample. The immersion corrosion results confirm the above discussed effects of grain size on corrosion resistance and show obvious differences in corrosion performance of NC and CG Ni in different corrosion media.

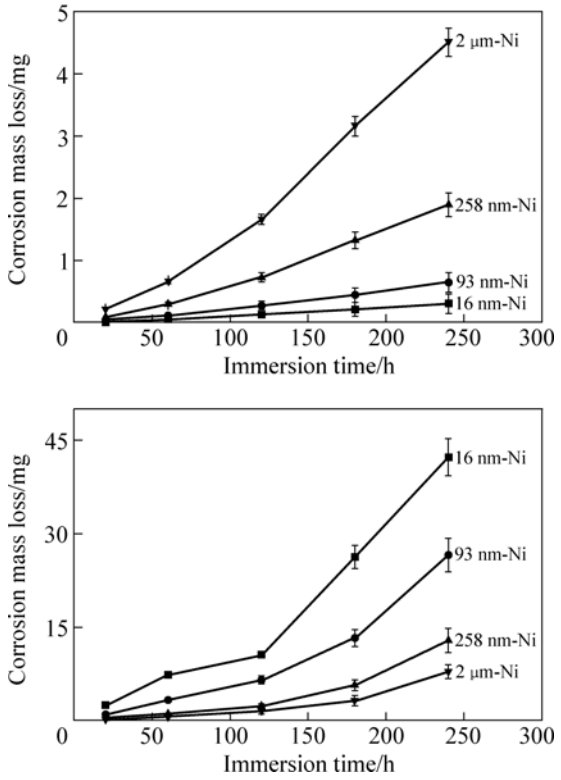

Fig.7 Mass loss curves of Ni deposits induced by immersion corrosion in 3% NaCl solution (a) and 1% H_2SO_4 solution (b)

4 Conclusions

1) By increasing the grain refiner (saccharin) concentration during direct current electrodeposition, CG Ni (2 μm) and NC Ni (16 nm to 258 nm) samples were fabricated.

2) Electrochemical corrosion and passivation behavior of the NC Ni deposits is of diffusion controlled mechanism and higher grain boundary density in NC materials strongly affects its corrosion behavior.

3) In NaOH and NaCl solutions, NC Ni with smaller grain size exhibits improved corrosion resistance in comparison with CG Ni due to its higher grain boundary density, which could accelerate the formation of continuous and protective passive films. In the H_2SO_4 solution, the corrosion resistance of NC Ni deposits decreases with decreasing grain size due to no passive process.

4) Higher grain boundary density in NC Ni deposits will accelerate corrosion by providing high density of active sites for preferential attack when being exposed to such corrosive environment. The positive or negative effect of higher grain boundary density on corrosion resistance mainly depends on whether passive film forms on the surface of sample.

References

[1] KUMAR K S, van SWYGENHOVEN H, SURESH S. Mechanical behavior of nanocrystalline metals and alloys [J]. Acta Materialia, 2003, 51: 5743−5774.

[2] KIM H S, BUSH M B. The effects of grain size and porosity on the elastic modulus of nanocrystalline materials [J]. Nanostructured Materials, 1999, 11: 361−367.

[3] RENNER F U, STIERLE A, DOSCH H, KOLB D M, LEE T L, ZEGENHAGEN J. Initial corrosion observed on the atomic scale [J]. Nature, 2006, 439: 707−710.

[4] LU K. Nanocrystalline metals crystallized from amorphous solids: Nanocrystallization, structure, and properties [J]. Materials Science and Engineering R, 1996, 16: 161−221.

[5] YOUSSEF KH M S, KOCH C C, FEDKIW P S. Improved corrosion behavior of nanocrystalline zinc produced by pulse-current electrodeposition [J]. Corrosion Science, 2004, 46: 51−64.

[6] YU B, WOO P, ERB U. Corrosion behaviour of nanocrystalline copper foil in sodium hydroxide solution [J]. Scripta Materialia, 2007, 56: 353−356.

[7] KIM S H, AUST K T, ERB U, GONZALEZ F, PALUMBO G. A comparison of the corrosion behaviour of polycrystalline and nanocrystalline cobalt [J]. Scripta Materialia, 2003, 48: 1379−1384.

[8] ALEDRESSE A, ALFANTAZI A. A study on the corrosion behavior of nanostructured electrodeposited cobalt [J]. Journal of Materials Science, 2004, 39: 1523−1526.

[9] ROFAGHA R, LANGER R, EL-SHERIK A M, ERB U, PALUMBO G, AUST K T. The corrosion behaviour of nanocrystalline nickel [J]. Scripta Metallurgica Materialia, 1991, 25: 2867−2872.

[10] MISHRA R, BALASUBRAMANIAM R. Effect of nanocrystalline grain size on the electrochemical and corrosion behavior of nickel [J]. Corrosion Science, 2004, 46: 3019−3029.

[11] GU C D, LIAN J S, HE J G, JIANG Z H. High corrosion-resistance nanocrystalline Ni coating on AZ91D magnesium alloy [J]. Surface and Coatings Technology, 2006, 200: 5413−5418.

[12] MISHRA R, BASU B, BALASUBRAMAMIAM R. Effect of grain size on the tribological behavior of nanocrystalline nickel [J]. Materials Science and Engineering A, 2004, 373: 370−373.

[13] QIN L Y, XU J Y, LIAN J S, JIANG Z H, JIANG Q. A novel electrodeposited nanostructured Ni coating with grain size gradient distribution [J]. Surface and Coatings Technology, 2008, 203: 142−147.

[14] ABRAHAM M, HOLWAY P, THUVANDER M, CAREZO A, SMITH G D W. Thermal stability of electrodeposited nanocrystalline nickel [J]. Surface Engineering, 2002, 18: 151−156.

[15] KISHIMOTO K, YOSHIOKA S, KOBAYAKAWA K, SATO Y. Effects of various additives on the characteristic of electrodeposited nickel thin film [J]. Journal of the Surface Finishing Society of Japan, 2003, 54: 710−713.

[16] LI Y, WANG F, LIU G. Grain size effect on the electrochemical corrosion behavior of surface nanocrystallized low-carbon steel [J]. Corrosion, 2004, 60: 891−896.

[17] WANG L P, ZHANG J Y, GAO Y, XUE Q J, HU L T, XU T. Grain size effect in corrosion behavior of electrodeposited nanocrystalline Ni coatings in alkaline solution [J]. Scripta Materialia, 2006, 55: 657−660.

[18] MACHET A, GALTAYRIES A, ZANNA S, KLEIN L, MAURICE V, JOLIVET P, FOUCAULT M, COMBRADE P, SCOTT P, MARCUS P. XPS and STM study of the growth and structure of passive films in high temperature water on a nickel-base alloy [J]. Electrochimica Acta, 2004, 49: 3957−3964.

[19] BADAWY W A, AL-KHARAFI F M, AL-AJMI J R. Electrochemical behaviour of cobalt in aqueous solutions of different pH [J]. Journal of Applied Electrochemistry, 2000, 30: 693−704.

[20] MATIENZO J, YIN L I, GRIM S O, SWARTZ W E. X-ray photoelectron spectroscopy of nickel compounds [J]. Inorganic Chemistry, 1973, 12: 2762−2769.

[21] THUBE M G, KULKARNI S K, HUERTA D, NIGAVEKAR A S. X-ray-photoelectron-spectroscopy study of the electronic structure of Ni-P metallic glasses [J]. Physical Review B, 1986, 34: 6874−6879.

[22] FURSTENAU R P, MCDOUGALL G, LANGELL M A. Initial stages of hydrogen reduction of NiO(100) [J]. Surface Science, 1985, 150: 55−57.

[23] BAI A, CHUAN P Y, HU C C. The corrosion behavior of Ni-P deposits with high phosphorous contents in brine media [J]. Materials Chemistry and Physics, 2003, 82: 93−100.

[24] BALYANOV A, KUTNYAKOVA J, AMIRKHANOVA N A, STOLYAROV V V, VALIEV R Z, LIAO X Z, ZHAO Y H, JIANG Y B, XU H F, LOWE T C, ZHU Y T. Corrosion resistance of ultra fine-grained Ti [J]. Scripta Materialia, 2004, 51: 225−229.

(Edited by YANG Hua)